Micro-structured polymer scaffolds fabricated by direct laser writing for tissue engineering

Paulius Danilevicius,[a] Sima Rekstyte,[a] Evaldas Balciunas,[b] Antanas Kraniauskas,[c] Rasa Jarasiene,[b] Raimondas Sirmenis,[c] Daiva Baltriukiene,[b] Virginija Bukelskiene,[b] Roaldas Gadonas,[a] and Mangirdas Malinauskas[a]
[a]Vilnius University, Faculty of Physics, Department of Quantum Electronics, Laser Research Center, Sauletekio Avenue 10, LT-10223 Vilnius, Lithuania
[b]Vilnius University, Institute of Biochemistry, Vivarium, Mokslininku Str. 12, LT-08662 Vilnius, Lithuania
[c]Vilnius University, Hospital Santariskiu Klinikos, Heart Surgery Center, Santariskiu Str. 2, LT-08661 Vilnius, Lithuania

Abstract. This work presents the latest results on direct laser writing of polymeric materials for tissue engineering applications. A femtosecond Yb:KGW laser (300 fs, 200 kHz, 515 nm) was used as a light source for non-linear lithography. Fabrication was implemented in various photosensitive polymeric materials, such as: hybrid organic-inorganic sol-gel based on silicon-zirconium oxides, commercial ORMOCER® class photoresins. These materials were structured via multi-photon polymerization technique with submicron resolution. Porous three-dimensional scaffolds for artificial tissue engineering were fabricated with constructed system and were up to several millimeters in overall size with 10 to 100 μm internal pores. Biocompatibility of the used materials was tested in primary rabbit muscle-derived stem cell culture *in vitro* and using laboratory rats *in vivo*. This interdisciplinary study suggests that proposed technique and materials are suitable for tissue engineering applications. [DOI: 10.1117/1.JBO.17.8.081405]

Keywords: direct laser writing; multi-photon polymerization; 3D scaffolds; biocompatible photopolymers; cardiovascular grafts; stem cell; tissue engineering.

Paper 11786SS received Dec. 23, 2011; revised manuscript received Mar. 12, 2012; accepted for publication Mar. 21, 2012; published online May 15, 2012.

1 Introduction

The interdisciplinary field of Tissue Engineering (TE) science has gained a lot of attention during the past decades. The main efforts are concerned with building artificial tissues or organs *in vitro* using stem cells derived from the patient. To achieve this, it is important to mimic the composition and structure of the original tissues.[1] The microporous structures are designed to serve as artificial niches for cell growing, and their well-defined geometrical shape can function as a biomimetic substrate. Chemical and geometrical properties of the scaffolds play an important role in regulating cell fate-their proliferation and differentiation.[2] Different chemical composition of biomaterials can direct differentiation of the stem cells into bone, skin, muscle or vascular tissues.[3–5] Cell growth, function and fate are closely related to geometrical properties of the scaffolds.[6,7] The critical processes governing artificial tissue integration such as cell migration and hybrid tissue organization are also dependent on scaffold geometrical properties such as pore size and general porosity.[8] Biomimetic properties of the scaffolds can be improved by immobilizing functional extracellular matrix (ECM) proteins onto the surface. Proteins-coated scaffolds can improve cell attachment and proliferation.[9,10] However, there are still many unresolved issues. It is also very important to have a better understanding of cell-surface interactions in order to successfully apply artificially engineered scaffolds in practical TE.

There is a variety of materials which have been used for scaffold production for TE applications. Generally they can be divided into natural and synthetic ones. Natural protein or polysacharide-based biomaterials, such as collagen,[11] gelatin,[12] fibrin,[13] silk,[14] chitosan[15] and alginate[16] are attractive because they have cellular adhesion sites and tend to be biocompatible. The disadvantages of these materials are poor mechanical properties and difficulties to ensure material purity and precise chemical composition. As an alternative to natural, synthetic biomaterials offer many advantages including mechanical stability, reproducibility due to precisely controlled chemical composition, ability to control degradation rate and other bioactivity properties. Those usually are polymer-based materials, such as poly (ethylene glycol),[17] poly (lactic-co-glycolic acid),[18] polycaprolactone,[19] polyester[20] and many other derivatives. However, some of these materials lack cell adhesion sites and may not be suitable for long-lasting implantation *in vivo* due to production of byproducts.[3] Nevertheless, there are ways to modify the surface of synthetic grafts in order to have desirable biomimetic properties.[21,22] Recently sol-gel prepared organic-inorganic hybrids received interest as biocompatible materials for medical devices.[23] The advantages of hybrid biomaterials are: straightforward preparation and modification, mechanical stability, and suitability for precise and high resolution structuring techniques of artificial scaffolds.[24]

To date there are many conventional fabrication techniques of scaffolds for TE. Several polymer processing techniques, such as fiber bonding,[25] solvent casting/particulate leaching,[26] gas foaming[27] and phase separation[28] involve either heating the polymers, dissolving them in particular solvents or applying high pressure gases. Most of them suffer from low mechanical strength and low pore interconnectivity.[29,30] A fabrication technique should be flexible enough to ensure various scaffold geometries, pore sizes and distribution. Rapid prototyping (RP)

Address all correspondence to: Mr. Malinauskas Mangirdas, Vilnius University, Faculty of Physics, Department of Quantum Electronics, Laser Research Center, Sauletekio Avenue 10, LT-10223 Vilnius, Lithuania. Tel: +370 60002843; Fax: +370 52366006; E-mail: mangirdas.malinauskas@ff.vu.lt

0091-3286/2012/$25.00 © 2012 SPIE

techniques offer the possibility of direct fabrication of computer-aided design (CAD) models which can have any geometry. Recently RP techniques, such as 3D printing,[31] selective laser sintering,[32] stereolithography[33] and fused deposition modeling[34] have attracted attention because they can produce scaffolds with controllable pore sizes, porosities, interconnectivity and mechanical strength. However, these methods suffer from limitations, which include low resolution, material restraints and relatively long processing times.

Direct laser writing (DLW) based on selective polymerization enables us to overcome most of the above mentioned limits. This technique is based on the structuring of polymers by a tightly focused laser beam. Polymerization reaction confined in a femtoliter volume focal spot is induced via non-linear absorption. This allows reaching structuring resolution of up to tens of nanometers.[35] By moving the beam three-dimensionally in the volume of pre-polymer one can create structures with no geometrical restraints.[36] Due to its exclusive advantages, multi-photon polymerization has already established its applications in fabrication of photonics,[37] microoptics,[38] microfluidics[39] as well as biomedical devices.[23,40]

In this work we present the latest results of DLW application in TE by fabricating 3D artificial scaffolds for stem cell growing out of hybrid organic-inorganic biomaterials. Critical parameters for high throughput fabrication were defined and high quality structures were fabricated. Scaffolds which are up to several millimeters in size had internal pore sizes of tens of micrometers with controllable general porosities. Furthermore, hybrid materials were tested for stem cell response *in vitro* and tissue response *in vivo*. Overall interdisciplinary study shows the advantages of DLW application in tissue engineering.

2 Methodology

2.1 *Photosensitive Polymer Materials*

Three different hybrid organic-inorganic polymer materials were used in our experiments. Two of them are commercially available UV curable materials Ormoclear and Ormocore b59 produced for photo-lithographic applications in microoptics (Micro Resist Technology GmbH). These materials belong to the ORMOCER class hybrid polymers and they are produced using sol-gel process from liquid precursors. They include inorganic oxide units and cross-linkable organic moieties such as urethane-and thioether (meth)-acrylate alkoxysilanes, and contain strong covalent bonds between the inorganic and organic components.[41] These materials were used as purchased without any further modifications (photoinitiatior is already added by the suppliers). These materials have been tested for scaffold production with DLW and biocompatibility before.[42] Another material is a two composite sol-gel based on zirconium and silicon oxides (SZ2080). The preparation of it is described elsewhere.[43] It contains inorganic silicon alkoxide and zirconium alkoxide groups which enhance materials mechanical stability, while organic part of SZ2080 contains polymerizable methacrylate moieties. This low shrinkage photopolymer was initially used to fabricate photonic elements,[44] but also found its applications in TE.[24]

SZ2080 was photosensitized by adding 1 to 2 wt. % of 2-Benzyl-2-dimethylamino-1-(4-morpholinophenyl)buta-none-1 photoinitiator (also known as Irgacure 369) (Sigma-Aldrich GmbH). This commercial photoinitiator was chosen because it has already been proved for suitability for high quality and throughput fabrication via DLW.[45,46] Although common commercial photoinitiators may suffer from low two-photon absorption efficiency[47] compared to the novel custom-made chromophores,[48,49] yet preparation of organic molecules with large two-photon absorption cross sections is rather complicated and was not involved in this research.

Before fabrication samples were prepared by drop-casting the materials on the microscope cover glass substrates. After laser processing the photosensitive resins exposed to light underwent polymerization and became insoluble in the developer [Fig. 1(a)]. Samples were treated with the appropriate organic solvent in order to wash out unexposed material. Polymerized structures sustained during the development process. In this way, the free-standing structures were fabricated on a glass substrate. Scanning Electron Microscopy (SEM) and optical profilometry were applied to evaluate the micro-structured scaffolds.

2.2 *Direct Laser Writing Setup and Scaffold Fabrication*

The schematics of the DLW system used in this work is depicted in Fig. 1(b). High peak power femtosecond Yb:KGW laser

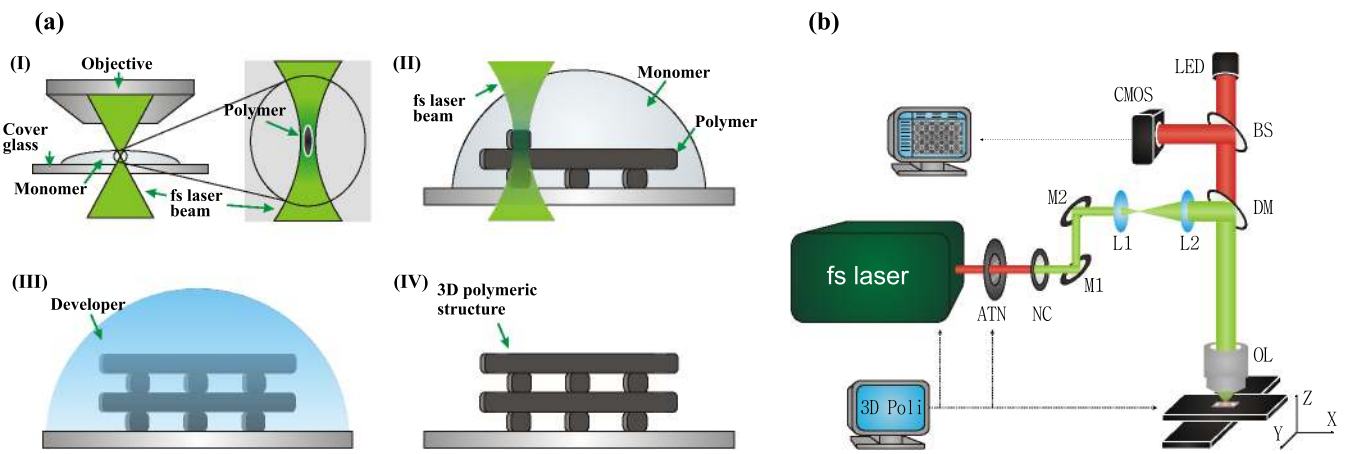

Fig. 1 (a) Fabrication steps: (I) photopolymerization reaction is initiated in the focal spot of the beam, (II) polymeric structure is directly written by moving the sample in regard to the focal spot, (III) organic developer washes unexposed material (IV) 3D free-standing scaffold is obtained on a glass substrate; (b) DLW fabrication setup: ATN-attenuator, NC-second harmonic non-linear crystal, M1-M2-mirrors, L1-L2-telescope, DM-dichroic mirror, OL-objective lens, BS-beam splitter, CMOS-camera.

amplifier (Pharos, Light Conversion Co. Ltd.) was used as irradiation source. Its parameters are: 300 fs pulse duration, 200 kHz repetition rate, 1030 nm central wavelength (515 nm second harmonic was used in experiment). 1 to 10 mW of average laser power was used which corresponds to $0.32 - 3.2\ \mathrm{TW/cm^2}$ (values are calculated assuming that 10×0.3 NA objective was used, which was the most practical for the fabrication of the scaffolds in our experiment).

Irradiation was calculated using $I_p = \frac{TE_p}{\tau_p \pi \omega}$,[50] where T is the objective's transmittance for 515 nm, $E_p = P/f$ is the pulse energy, τ_p is the pulse duration and $\omega_p = \frac{0.61\lambda}{\mathrm{NA}}$ is the beam waist radius. For the highest translation velocity achieved we calculated the cumulative dose of exposure $D_{ac} = D_p \times N_p$, where D_p is the dose per pulse ($D_p = I_p \tau_p$) and N_p is the number of pulses per focal spot. The estimated cumulative dose was $4.6\ \mathrm{J/cm^2}$ showing an efficient energy use for polymerization reaction when using fs pulses. All necessary values used for calculations and calculated quantities are given in Table 1.

The laser beam was guided through an optical system [Fig. 1(b)] to a high numerical aperture objective and focused to a volume of photopolymer. The sample was mounted on high speed and wide working area positioning system which consisted of linear motor driven stages (Aerotech, Inc.): XY-ALS130 to 100, Z-ALS130 to 50. These stages ensure an overall traveling range of 100 mm in X and Y directions and 50 mm in Z direction and support the scanning velocity of up to 300 mm/s while keeping positioning resolution up to 10 nm. Upon irradiation the monomers underwent transition from liquid to solid (or from gel to solid) which resulted in the change of the refractive index. It enabled wide-field transmission microscopy to be used for monitoring the manufacturing process in real time. A microscope was built by adding its main components to the system: a source of red light provided by a LED, a CMOS camera (mvBlueFOX-M102G, Matrix Vision GmbH) and a video screen. The ability to image photostructuring while performing DLW is an important feature for a successful fabrication process. Control of all equipment was automated via custom-made software 3DPoli specially designed for DLW applications.* By moving the sample three-dimensionally, the position of the laser focus was being changed inside the resin and this enabled writing of complex 3D structures. Structures can be imported from CAD files or programmed directly. This DLW system was tested for structuring in various photosensitive materials at large scale. The ability to scale up and speed up the fabrication was ensured by changing the laser beam focusing objectives in the range from $100 \times \mathrm{NA} = 1.4$ to $10 \times \mathrm{NA} = 0.3$, thus at the sacrifice of the resolution from 200 nm to 4 μm.[51]

Table 1 Fabrication parameters (NA-objective's numerical aperture, λ-laser radiation wavelength, τ_p-pulse duration, f-pulse repetition rate, T-objective's transmittance for 515 nm, υ-sample scanning velocity, P-average laser power, ω-beam waist radius, E_p-pulse energy, I_p-irradiation, N_p-number of pulses per focal spot, D_p-dose per pulse, D_{ac}-cumulative dose).

Quantity	Value	Calculated quantity	Value
NA	0.3	ω	1.05 μm
λ	515 nm	E_p	20 nJ
τ_p	300 fs	I_p	1.3 TW/cm^2
f	200 kHz	N_p	12
T	66.5%	D_p	0.38 J/cm^2
υ	35 mm/s	D_{ac}	4.6 J/cm^2
P	4 mV		

2.3 *Biocompatibility Tests In Vitro and In Vivo*

Biocompatibility of the micro-structured materials was assessed *in vitro* using stem cell culture and *in vivo* using laboratory rats (Lithuanian State Food and Veterinary Office license for use of laboratory animals for scientific research work No. 0212, 2011 to 02-04). Laboratory rats were taken care of according to the Lithuanian Law on animal care, housing and use (No. VIII-500, 1997 to 11-06).

For the studies *in vitro*, a primary myogenic stem cell line derived from adult rabbit skeletal muscle was established.[52] Before cell seeding, the specimens were sterilized with 70% ethanol for 24 h, and dried on a clean bench under UV irradiation. The cells were grown in Iscoves modified Dulbeccos medium (Sigma-Aldrich GmbH) supplemented with 10% fetal calf serum (Biological Industries Ltd.) and antibiotics (penicillin, 100 U/ml, streptomicin, 100 μg/ml; Biological Industries Ltd.), at 37°C and 5% CO_2. For the evaluation of biocompatibility, the cells (6×10^4/ml) were grown for 48 h on the tested micro-structured polymeric scaffolds which were placed inside the wells of a 24-well plate (Orange Scientific). Cell viability was examined using differentiating staining with acridine orange (AO, 100 μg/ml, Molecular Probes Inc.) and etidium bromide (EB, 100 μg/ml, Sigma-Aldrich GmbH).[53] 4 μl of AO/EB dye mixture (1:1) was added to 100 μl of growth medium on the cell monolayer. Fluorescent microscopy (Nikon Instruments Inc.) analysis allows to distinguish living (green) and dead (orange) cells in cell population stained this way. On the basis of cell membrane integrity, AO binds to DNA of viable cells and stains them green, as well, EB bounds to the DNA of nonviable cells and stain them in orange.

In vivo study was performed by using healthy male Wistar rats, weighting 250 to 300 g (Vivarium of the Institute of Biochemistry, Vilnius University). Prior to the surgery, the polymeric structures out of Ormocore b59 and SZ2080 were washed in ethanol (3×24 h) and dried under UV (2×15 min, both sides). The rats were anesthetized by intramuscular injection of ketamine hydrochloride (100 mg/ml; 40 mg/kg) (Vetoquinol Biowet, Poland) and xylazine hydrochloride (2%; 5 mg/kg) (Bela-pharm, Germany). The lumbar area of the rat was prepared aseptically for surgery, longitudinal incisions of approximately 1 cm were made in the skin near the paravertebral back muscle where two samples of each polymer were inserted. The incisions were closed with interrupted sutures of Polysorb 4 to 0 suture (Syneture). After 3 weeks, the animals were euthanized, each implant was removed and a histological analysis of the surrounding tissues was performed in the National Center of Pathology (Vilnius, Lithuania). Biocompatibility of the tested polymeric samples was evaluated judging by the microscopic views of the histologic specimens of surrounding tissues stained with hematoxylin and eosin (H&E).

*3DPoli@gmail.

3 Results

3.1 *Fabrication of 3d Scaffolds*

One of the most important advantages of DLW compared to alternative above mentioned technologies is the precise control of structuring resolution, which allows fabricating precise objects with almost no geometrical restraints. Spatial resolution can be flexibly tuned by varying laser output power and translation velocity of the sample, by replacing focusing objectives or by altering sensitivity of the material itself (changing the concentration of the used photoinitiator).

To the best of our knowledge up to date, the structure shown in Fig. 2 is the largest 3D micro-structured scaffold produced by femtosecond direct laser writing in polymers.[54]

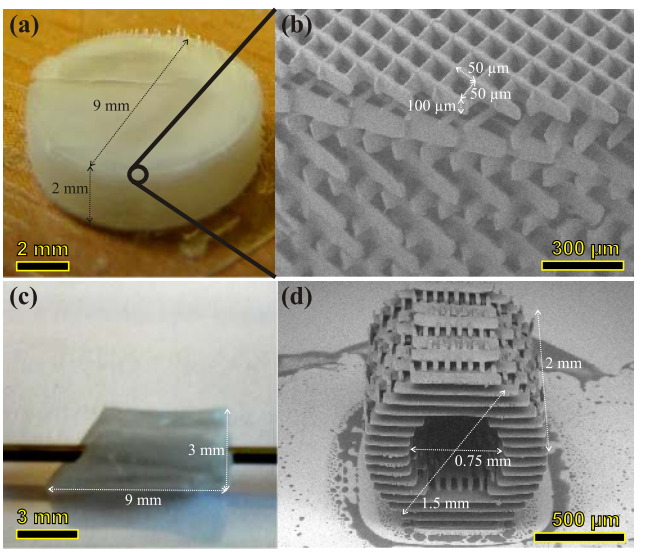

Fig. 2 (a) A photo of $9 \times 9 \times 2$ mm^3 disc shape scaffold out of SZ2080 polymer; (b) Inset shows SEM image of internal structure of the disc shape scaffold. The pore size is $50 \times 50 \times 100$ μm^3, and the general porosity is 60%. 5 mm/s sample translation velocity and 10×0.3 NA objective were used; (c) A photo of an artificial blood vessel scaffold out of Ormoclear polymer with outer diameter of 3 mm, internal diameter 1.5 mm, length of 9 mm and a 45° cut edge. The pore size is $10 \times 10 \times 100$ μm^3, and the general porosity is 67%. 10 mm/s sample translation velocity and $10 \times$ 0.3 NA objective lens were used; (d) SEM image of an artificial blood vessel scaffold fabricated out of Ormoclear polymer with a 1.5 mm outer diameter and a 0.75 mm internal diameter with a length of 2 mm. The pore size is $50 \times 50 \times 100$ μm^3, and the general porosity is 50%. 2 mm/s sample translation velocity and $10 \times$ 0.3 NA objective lens were used.

3.2 *Biocompatibility Test of Hybrid Materials*

The biocompatibility of micro-structured polymeric scaffolds fabricated out of Ormocore b59 and SZ2080 was evaluated *in vitro* using rabbit muscle-derived myogenic cells which were grown on the tested materials. Polystyrene was used as a control surface. The results demonstrate that the viability of cells grown on polymeric scaffolds is comparable to that on control surfaces. In both cases, less than ten percent of dead cells were found (Fig. 3).

For the biocompatibility studies *in vivo*, after three weeks of implantation, histological analysis of tissues surrounding the implant was performed. It is known that the presence of the implant changes the healing process. A reaction of biological tissue to any foreign material is called the Foreign-Body Reaction (FBR). Foreign bodies can be inert or irritating, some of them can be toxic and cause inflammation as well as scarring. The normal FBR consists of macrophages and foreign-body giant cells at the surface of the implant with subjacent fibroblastic proliferation and collagen deposition, and capillary formation. Macrophages play a pivotal role in the response of tissue to implants.[55] As revealed in the Fig. 4, a mild FBR, characterized by the sporadic presence of macrophages and lymphocytes, is observed in the tested slides. Taking into account that such tissue reaction is registered three weeks after the implantation, the results are considered to be positive and demonstrate that tested materials were non-cytotoxic and biocompatible, showing them to be suitable for biomedical practice.

Comparing test results *in vitro* and *in vivo* we conclude that studied polymeric structures are biocompatible and suitable for tissue engineering applications.

4 Discussion

Advances in regenerative medicine would not have been possible without the innovative biomaterials, which provide the structural framework for cells to form tissues and synthesize extracellular matrices.[56,57] Herein we have successfully fabricated large scale scaffolds from the hybrid polymeric materials and demonstrated the possibility to control scaffold geometry, porosity and pore size at micro-scale. An organic-inorganic sol-gel based on silicon-zirconium oxides and commercial ORMOCER® class photoresins were subjected to DLW. ORMOCERs are successfully used in high-tech industries, such as optical coatings, electronics, and medical technology, especially dentistry.[58] An inorganic part of ORMOCER molecule is represented by silica network and is produced through targeted hydrolysis and inorganic polycondensation in a sol-gel process. (Meth)acrylate organic groups form a highly cross-linked network matrix after induction of a radical-based

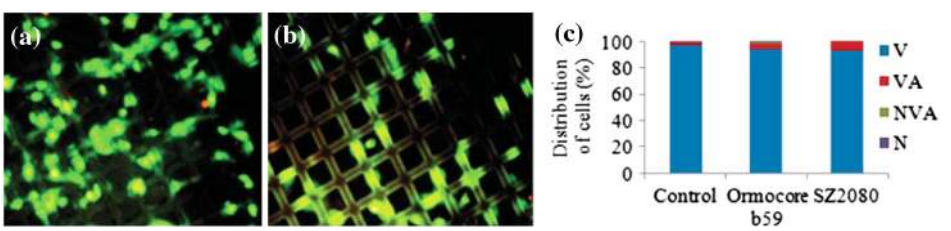

Fig. 3 Living rabbit muscle-derived myogenic stem cells growing *in vitro* on the micro-structured Ormocore b59 (a) and SZ2080 (b) polymeric surfaces. (c) The distribution of viable and non-viable cells growing on tested surfaces according to AO/EB staining. Cells were categorized as follows: V-viable with non-fragmented nuclei (bright green chromatin); VA-viable with fragmented nuclei (bright green chromatin with organized structure); N necrotic (red non-fragmented nuclei); NVA-non-viable apoptotic with fragmented nuclei (bright orange chromatin that is highly condensed or fragmented). Chromatin-free cells lost their DNA content entirely and exhibited weak green-orange staining.[53]

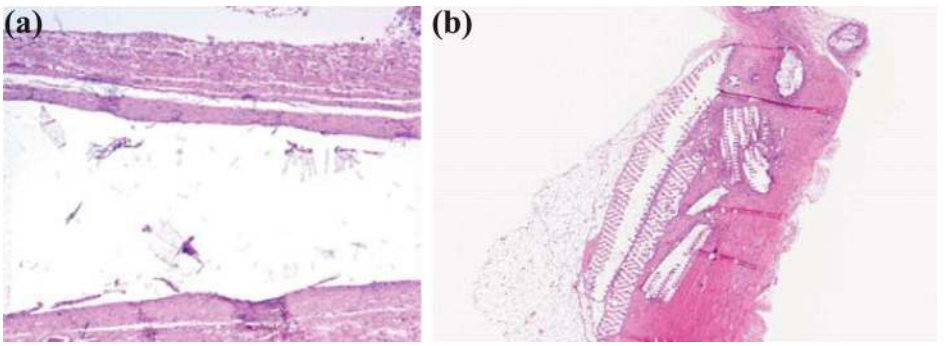

Fig. 4 Biocompatibility tests *in vivo*: (a) tissue reaction to the nonstructured Ormoclear and (b) to micro-structured SZ2080; mild FBR, characterized by a small number of macrophages and lymphocytes around the implant location is observed in the tested slides.

polymerization.[59,60] It is supposed that the abundance of polymerization opportunities in these materials determine the low amount of uncrosslinked monomers and therefore better biocompatibility. However, only limited information is available about the elution of monomers from ORMOCERs and their toxicity.[61] Hybrid methacrylates based on silane derivates (ORMOSILs) also exhibit properties originating from both of their organic and inorganic chemical groups.[62] A way to circumvent the use of methacrylate-based photopolymers, that sometimes suffer from cytotoxicity, new monomers based on vinyl esters were prepared and tested,[63] which might be will become more widely used for DLW targeted bio-applications in the near future.

In our experiment we used three different hybrid polymers: ORMOCER® class photoresins-Ormocore b59 and Ormoclear as well as a two composite sol-gel based on zirconium and silicon oxides-SZ2080. Sample translation speeds of up to 35 mm/s were achieved using Ormocore b59 hybrid polymer. Such velocity allows to fabricate a disk shaped scaffold of 2 mm height and 18 mm diameter or an artificial blood vessel scaffold with 9 mm outer diameter, 4.5 mm internal diameter and 8 mm height just overnight. It corresponds to polymerization of a 1 cm^3 volume structure, assuming that a cube with 1 cm sides and a fill factor of 30% is fabricated. The rectangular form eliminates the losses due to circular shape and hollow core of blood vessel which results in not all scanning time being used for polymerization as scanning through hollow parts is done with a closed shutter. It is also important to mention, that fabrication time depends on the fill factor of the structure, since lower fill factor requires less scanning time.

As calculated in Table 1, DLW employing femtosecond lasers allows one to microstructure using light exposure doses within the therapeutic range ($1-10$ J/cm^2). Having the sufficient light density for the irreversible photomodification one can think of artificial scaffold creation during *in vitro* tests[64] and, due to already achieved high fabrication throughput, even during *in vivo* surgery.[65] This would enable dynamic experiments of cell proliferation or creation of custom shaped artificial scaffolds in real time.

Polymeric scaffolds used in regenerative medicine react with physiological fluids and through cellular activity form tenacious bonds to hard and in some cases to soft tissues.[66] However, their biocompatibility and biodegradability are often insufficient, limiting their potential clinical use. In our experiments, the obtained data showed high viability of stem cells grown on non-degradable polymeric scaffolds constructed by direct laser writing. In another study, productive interaction of fibroblasts with two epidermal cell types was found during their growth on Ormosil scaffolds fabricated by two-photon polymerization.[67] Therefore, this procedure proves to be a relatively simple method for processing of polymeric scaffolds and designing an initial environment for cell growth.

According to our data, the polymeric scaffolds can guide cell orientation and grouping; the cellular behavior being influenced by the surrounding microenvironment. The scaffold allows the cells to migrate to their surroundings and it can act as a structure where the cells are made to grow in a programmed way. The produced scaffolds are biocompatible and easily processable, making them suitable for tissue engineering and medical applications.

5 Conclusions

After completion of this synergetic laser-scaffold-fabrication and biocompatibility study, the following conclusions can be drawn:

1. Adult myogenic stem cell proliferation tests on polymeric substrates show that the selected laser 3D microstructurable materials, such as Ormocore b59, Ormoclear and SZ2080, are applicable for biomedical tissue engineering practice. It is supported by *in vivo* biocompatibility tests of these polymer materials implanted in living rats organisms. The obtained results are encouraging for the future work toward using these materials for cell growing, tissue engineering and soft or hard tissue regeneration applications.
2. The flexible direct laser writing approach for the production of custom shape and pore size as well as porosity polymeric scaffolds has reached the level of fabrication throughput requisite for practical applications. True 3D micro-structured scaffolds of sizes up to 1 cm^3 and pore sizes in the range of $10-100$ μm with controlled porosity can be manufactured overnight, thus be created for an individual patient once required. Precise control of the form and filling factor of the artificial scaffold enables one to control its mechanical properties. For the direct laser writing technology this is the step out of the laboratory to the market.
3. Using high pulse repetition femtosecond lasers operating at the visible wavelengths the exposure dose

needed for the localized photopolymerization does not exceed the values tolerable for performing *in vitro* and *in vivo*. This opens a unique way to photostructure the scaffolds in real time during the cell proliferation or surgery experiments.

Further experiments are targeted toward using elastic or biodegradable and additionally biologically functionalized materials for the creation of artificial scaffolds with desired properties.

Acknowledgments

This work was supported by the Lithuanian State Science and Studies Foundation Grant No. MIP-10344. We gratefully acknowledge Dr. M. Farsari (Foundation of Research and Technology Hellas, Greece, mfarsari@iesl.forth.gr) for providing zirconium containing sol-gel hybrid photosensitive material SZ2080.

References

1. E. Lavik and R. Langer, "Tissue engineering: current state and perspectives," *Appl. Microbiol. Biotechnol.* **65**(1), 1–8 (2004).
2. Y. Li and S. T. Yang, "Effects of three-dimensional scaffolds on cell organization and tissue development," *Biotechnol. Bioproc. Eng.* **6**(5), 311–325 (2001).
3. S. Willerth and S. Sakiyama-Elbert, "Combining stem cells and biomaterial scaffolds for constructing tissues and cell delivery," *Stem Book*, Harvard Stem Cell Institute, Cambridge, MA(2008).
4. S. Levenberg et al., "Differentiation of human embryonic stem cells on three-dimensional polymer scaffolds," *Proc. Natl. Acad. Sci. USA* **100**(22), 12741–12746 (2003).
5. J. George, Y. Kuboki, and T. Miyata, "Differentiation of mesenchymal stem cells into osteoblasts on honeycomb collagen scaffolds," *Biotechnol. Bioeng.* **95**(3), 404–411 (2006).
6. G. Kumar et al., "The determination of stem cell fate by 3D scaffold structures through the control of cell shape," *Biomaterials* **32**(35), 9188–9196 (2011).
7. A. Graziano et al., "Scaffolds surface geometry significantly affects human stem cell bone tissue engineering," *J. Cell Physiol.* **214**(1), 166–172 (2008).
8. S. Peyton et al., "Marrow-derived stem cell motility in 3d synthetic scaffold is governed by geometry along with adhesivity and stiffness," *Biotechnol. Bioeng.* **108**(5), 1181–1193 (2011).
9. E. Yildirim et al., "Accelerated differentiation of osteoblast cells on polycaprolactone scaffolds driven by a combined effect of protein coating and plasma modification," *Biofabrication* **2**(1), 014109 (2010).
10. V. Sales et al., "Protein precoating of elastomeric tissue-engineering scaffolds increased cellularity, enhanced extracellular matrix protein production, and differentially regulated the phenotypes of circulating endothelial progenitor cells," *Circulation* **116**, I-55–I-63 (2007).
11. J. Glowacki and S. Mizuno, "Collagen scaffolds for tissue engineering," *Biopolymers* **89**(5), 338–344 (2008).
12. A. Ovsianikov et al., "Laser fabrication of three-dimensional CAD scaffolds from photosensitive gelatin for applications in tissue engineering," *Biomacromolecules* **12**(4), 851–858 (2011).
13. W. Bensaid et al., "A biodegradable fibrin scaffold for mesenchymal stem cell transplantation," *Biomaterials* **24**(14), 2497–2502 (2003).
14. R. Nazarov, H. Jin, and D. Kaplan, "Porous 3-D scaffolds from regenerated silk fibroin," *Biomacromolecules* **5**(3), 718–726 (2004).
15. C. Ji et al., "Fabrication of porous chitosan scaffolds for soft tissue engineering using dense gas co_2," *Acta Biomaterials* **7**(4), 1653–1664 (2011).
16. N. Mohan and P. Nair, "Novel porous, polysaccharide scaffolds for tissue engineering application," *Trends Biomater. Artif. Organs* **18**(2), 219–224 (2005).
17. A. Ovsianikov et al., "Three-dimensional laser micro- and nano-structuring of acrylated poly(ethylene glycol) materials and evaluation of their cytoxicity for tissue engineering applications," *Acta Biomater.* **7**(3), 967–974 (2011).
18. W. Koegler and L. Griffth, "Osteoblast response to PLGA tissue engineering scaffolds with PEO modified surface chemistries and demonstration of patterned cell response," *Biomaterials* **25**(14), 2819–2830 (2003).
19. H. Kweon et al., "A novel degradable polycaprolactone networks for tissue engineering," *Biomaterials* **24**(5), 801–808 (2003).
20. F. Migneco et al., "Poly(glycerol-dodecanoate), a biodegradable polyester for medical devices and tissue engineering scaffolds," *Biomaterials* **30**(33), 6479–6484 (2009).
21. Y. Jiao and F. Cui, "Surface modification of polyester biomaterials for tissue engineering," *Biomed. Mater.* **2**(4), R24–R37 (2007).
22. K. Wulf et al., "Surface functionalization of poly(e-caprolactone) improves its biocompatibility as scaffold material for bioartificial vessel prostheses," *J. Biomed. Mater. Res. B* **98B**(1), 89–100 (2011).
23. A. Doraiswamy et al., "Two photon induced polymerization of organicinorganic hybrid biomaterials for microstructured medical devices," *Acta Biomater.* **2**(3), 267–275 (2006).
24. S. Psycharakis et al., "Tailor-made three-dimensional hybrid scaffolds for cell cultures," *Biomed. Mater.* **6**(4), 045008 (2011).
25. A. Mikos et al., "Preparation of poly(glycolic acid) bonded fiber structures for cell attachment and transplantation," *J. Biomed. Mater. Res.* **27**(2), 183–189 (1993).
26. A. Mikos et al., "Preparation and characterization of poly(l-lactic acid) foams," *Polymer* **35**(5), 1068–1077 (1994).
27. D. Mooney et al., "Novel approach to fabricate porous sponges of poly(d,l-lactic-co-glycolic acid) without the use of organic solvents," *Biomaterials* **17**(14), 1417–1422 (1996).
28. K. Whang et al., "A novel method to fabricate bioabsorbable scaffolds," *Polymer* **36**(4), 837–842 (1995).
29. C. Chua et al., "Development of a tissue engineering scaffold structure library for rapid prototyping. part 1: investigation and classification," *Int. J. Adv. Manuf. Technol.* **21**(4), 291–301 (2003).
30. A. Mikos and J. Temenoff, "Formation of highly porous biodegradable scaffolds for tissue engineering," *Electron. J. Biotechnol.* **3**(2), 1995–2000 (2000).
31. C. Lam et al., "Scaffold development using 3d printing with a starch-based polymer," *Mater. Sci. Eng. C Biomimetic Mater. Sensors Syst.* **20**(1–2), 49–56 (2002).
32. C. Chua et al., "Development of tissue scaffolds using selective laser sintering of polyvinyl alcohol/hydroxyapatite biocomposite for craniofacial and joint defects," *J. Mater. Sci. Mater. Med.* **15**(10), 1113–1121 (2004).
33. T. Matsuda, M. Mizutani, and S. Arnold, "Molecular design of photocurable liquid biodegradable copolymers. 1. synthesis and photocuring characteristics," *Macromolecules* **33**(3), 795–800 (2000).
34. I. Zein et al., "Fused deposition modeling of novel scaffold architectures for tissue engineering applications," *Biomaterials* **23**(4), 1169–1185 (2002).
35. S. Juodkazis et al., "Two-photon lithography of nanorods in su-8 photoresist," *Nanotechnology* **16**(6), 846–849 (2005).
36. M. Malinauskas et al., "3d artificial polymeric scaffolds for stem cell growth fabricated by femtosecond laser," *Lith. J. Phys.* **50**(1), 75–82 (2010).
37. S. Juodkazis, V. Mizeikis, and H. Misawa, "Three-dimensional microfabrication of materials by femtosecond lasers for photonics applications," *J. Appl. Phys.* **106**(5), 051101 (2009).
38. M. Malinauskas et al., "Femtosecond laser polymerization of hybrid/integrated micro-optical elements and their characterization," *J. Opt.* **12**(12), 124010 (2010).
39. D. Wu et al., "Femtosecond laser rapid prototyping of nanoshells and suspending components towards micro luidic devices," *Lab on a Chip* **9**(16), 2391–2394 (2009).
40. M. Malinauskas et al., "Large scale laser two-photon polymerization structuring for fabrication of artificial polymeric scaffolds for regenerative medicine," in *AIP Conf. Proc.*, Vol. **1288**, pp 12–17 (2010).
41. R. Buestrich et al., "ORMOCERs for optical interconnection technology," *J. Sol-Gel Sci. Technol.* **20**(2), 181–186 (2001).
42. S. Schlie et al., "Three-dimensional cell growth on structures fabricated from ORMOCER by two-photon polymerization technique," *J. Biomater. Appl.* **22**(3), 1–14 (2007).
43. A. Ovsianikov et al., "Two-photon polymerization of hybrid sol-gel materials for photonics applications," *Laser Chem.* **2008**, 493059 (2008).

44. A. Ovsianikov et al., "Ultra-low shrinkage hybrid photosensitive material for two-photon polymerization microfabrication," *ACS Nano.* **2**(11), 2257–2262 (2008).
45. M. Malinauskas et al., "Laser two-photon polymerization micro- and nanostructuring over a large area on various substrates," *Proc. SPIE* **7715**(77157F), 1–12 (2010).1
46. M. Malinauskas et al., "Mechanisms of three-dimensional structuring of photo-polymers by tightly focussed femtosecond laser pulses," *Opt. Express* **18** (10), 10209–10221 (2010).
47. K. Schafer et al., "Two-photon absorption cross-sections of common photoinitiators," *J. Photochem. Photobiol. A Chem.* **162**(2-3), 497–502 (2004).
48. M. Albota et al., "Design of organic molecules with large two-photon absorption cross sections," *Science* **281**(5383), 1653–1656 (1998).
49. N. Pucher et al., "Structure activity relationship in d-π-a-π-d-based photoinitiators for the two-photon-induced photopolymerization process," *Macromolecules* **42**(17), 6519–6528 (2009).
50. M. Malinauskas, P. Danilevicius, and S. Juodkazis, "Three-dimensional micro-/nano-structuring via direct write polymerization with picosecond laser pulses," *Opt. Express* **19**(6), 5602–5610 (2011).
51. M. Malinauskas et al., "Femtosecond visible light induced two-photon photopolymerization for 3D micro/nanostructuring in photoresists and photopolymers," *Lith. J. Phys.* **50**(2), 201–207 (2010).
52. V. Bukelskiene et al., "Muscle-derived primary stem cell lines for heart repair," *Semin. Cardiol.* **11**(3), 99–105 (2005).
53. S. Mercille and B. Massie, "Induction of apoptosis in nutrient-deprived cultures of hybridoma and myeloma cells," *Biotechnol. Bioeng.* **44**(9), 1140–1154 (1994).
54. T. Stichel et al., "Two-photon polymerization as method for the fabrication of large scale biomedical scaffold applications," *JLMN* **5**(3), 209–212 (2010).
55. J. Anderson, "Inflammatory response to implants," *ASAIO J.* **34**(2), 101–107 (1988).
56. M. Rahaman and J. Mao, "Stem cell-based composite tissue constructs for regenerative medicine," *Biotechnol. Bioeng.* **91**(3), 261–284 (2005).
57. B. Dhandayuthapani et al., "Polymeric scaffolds in tissue engineering application: a review," *Int. J. Polym. Sci.* **2011**1–19 (2011).
58. L. Cavalcante et al., "Degradation resistance of ormocer and dimethacrylate-based matrices with different filler contents," *J. Dent.* **40**(1), 86–90 (2012).
59. K. Haas and H. Wolter, "Synthesis, properties and applications of inorganicorganic copolymers (ORMOCER®s)," *Curr. Opin. Solid State Mater. Sci.* **4**(6), 571–580 (1999).
60. A. Sivakumar and A. Valiathan, "Dental ceramics and ormocer technology-navigating the future!," *Trends Biomater. Artif. Organs* **20**(1), 40–43 (2006).
61. O. Polydorou et al., "The effect of storage medium on the elution of monomers from composite materials," *J. Biomed. Mater. Res. B Appl. Biomater.* **100B**(1), 68–74 (2012).
62. A. Matei et al., "Laser processing of ormosils for tissue engineering applications," *Appl. Phys. A* **104**(3), 821–827 (2011).
63. C. Heller et al., "Vinyl esters: low cytotoxicity monomers for the fabrication of biocompatible 3D scaffolds by lithography based additive manufacturing," *J. Polym. Sci. A Polym. Chem.* **47**(24), 6941–6954 (2009).
64. K. Arcaute, B. K. Mann, and R. B. Wicker, "Stereolithography of three-dimensional bioactive poly(ethylene glycol) constructs with encapsulated cells," *Ann. Biomed. Eng.* **34**(9), 1429–1441 (2006).
65. J. Torgersen et al., "In vivo writing using two-photon-polymerization," *Proc. LPM2010*, Stuttgart, Germany (2010).
66. L. L. Hench, "Bioceramics," *J. Am. Ceram. Soc.* **81**(7), 1705–1727 (1998).
67. L. Sima et al., "Dermal cells distribution on laser-structured ormosils," *J. Tiss. Eng. Regen. Med.* (E-pub ahead of print) (2011).